ChemComm

COMMUNICATION

View Article Online
View Journal

Cite this: DOI: 10.1039/d1cc05879g

Received 19th October 2021,
Accepted 13th December 2021

DOI: 10.1039/d1cc05879g

rsc.li/chemcomm

Biophysical and *in silico* characterization of NrtA: a protein-based host for aqueous nitrate and nitrite recognition†

Ke Ji, [a] Kiheon Baek, [a] Weicheng Peng, [ab] Kevin A. Alberto, [a] Hedieh Torabifard, [a] Steven O. Nielsen *[a] and Sheel C. Dodani *[a]

Nitrate and nitrite are key components of the global nitrogen cycle. As such, Nature has evolved proteins as biological supramolecular hosts for the recognition, translocation, and transformation of both nitrate and nitrite. To understand the supramolecular principles that govern these anion-protein interactions, here, we employ a hybrid biophysical and *in silico* approach to characterize the thermodynamic properties and protein dynamics of NrtA from the cyanobacterium *Synechocystis sp. PCC 6803* for the recognition of nitrate and nitrite.

Nitrate and nitrite are essential inorganic anions connecting all forms of life and their environments.[1] In bacterial and plant cells, nitrate is a substrate for assimilatory and aerobic/anaerobic respiration pathways *via* the interconversion of nitrate, nitrite, and ammonium; in animal cells, nitrate and nitrite are thought to be storage reservoirs for nitric oxide homeostasis affording therapeutic potential.[2–6] Their natural distributions can be perturbed through anthropogenic means, particularly by excessive crop fertilization leading to water pollution and eutrophication, with detrimental biological consequences.[7,8] Across all these processes, cells must dynamically recognize, translocate, and transform these anions to maintain homeostasis.

Along these lines, Nature has evolved proteins as biological supramolecular hosts to form thermodynamically stable complexes with nitrate and/or nitrite in water.[9–17] Representative crystal structures for a subset of these proteins indicate that this recognition is achieved by combining the hydrophobic effect with cooperative hydrogen bonding, ion-pairing, and van der Waals interactions. These supramolecular designs are tailored to the properties of the anions, including size (nitrate: 179 pm; nitrite: 192 pm), shape (trigonal planar *vs.* bent), charge (monoanionic), basicity (nitrate < nitrite), and hydration enthalpy (nitrate: 310 kJ mol^{-1}; nitrite: 410 kJ mol^{-1}).[18] Indeed, protein-based hosts have served as the inspiration to design synthetic supramolecular hosts for nitrate and nitrite recognition, for which there are few aqueous examples.[19–23] To better inform this design, we are actively studying interactions between nitrate/nitrite and prokaryotic protein-based hosts as part of a larger program aimed at decoding the supramolecular principles of biological anion recognition.[24–26] Here, we have developed a hybrid workflow using isothermal titration calorimetry (ITC) and molecular dynamics (MD) simulations to dissect the thermodynamic contributions and protein motions of NrtA from the cyanobacterium *Synechocystis sp. PCC 6803* upon nitrate and nitrite binding.[9]

NrtA is a periplasmic solute binding lipoprotein of the ABC transport system NrtABCD that sequesters nitrate and nitrite from the environment (Fig. 1 left panel).[27,28] It delivers nitrate and nitrite from the periplasm to NrtB, an inner membrane

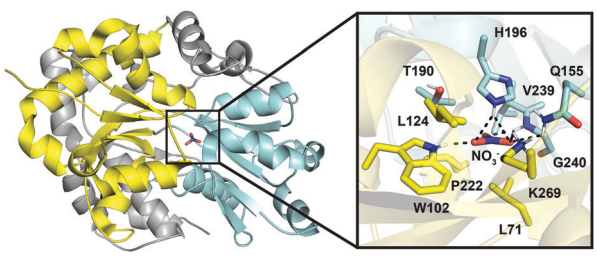

Fig. 1 X-ray crystal structure of nitrate-bound NrtA (residues 57–441, PDB ID: 2G29) from *Synechocystis sp. PCC 6803*. The two globular domains are highlighted in yellow and cyan (left). Residues within 4 Å of the nitrate ion are shown as sticks with all oxygen atoms in red, nitrogen atoms in blue, and hydrogen atoms in white (right). All known hydrogen bonding or electrostatic interactions with nitrate are shown with dashed lines. Each residue is labelled with the single letter amino acid abbreviation and corresponding sequence number.

[a] *Department of Chemistry and Biochemistry, The University of Texas at Dallas, Richardson, TX 75080, USA. E-mail: steven.nielsen@utdallas.edu, sheel.dodani@utdallas.edu*

[b] *Department of Biological Sciences, The University of Texas at Dallas, Richardson, Texas 75080, USA*

† Electronic supplementary information (ESI) available. See DOI: 10.1039/d1cc05879g

spanning protein that translocates the anions into the cytosol. The latter transport process is coupled to the hydrolysis of ATP through the action of the membrane associated partners NrtC and NrtD. Based on the crystal structure of the nitrate-bound form of NrtA from *Synechocystis sp. PCC 6803*, NrtA is composed of two globular domains that create a cleft for the nitrate binding site.[9] Inside the binding pocket, K269 serves as an anchor for nitrate binding and Q155, H196, and G240 provide additional hydrogen bonding interactions (Fig. 1 right panel). The binding pocket is also lined with L71, W102, L124, P222, and V239. Through the hydrophobic effect, these residues can also facilitate anion binding. Beyond these structural insights, the binding of nitrate and nitrite to NrtA from *Synechocystis sp. PCC 6803* has not been further characterized until this study. However, the dissociation constants (K_d) for nitrate and nitrite binding have been determined for two different homologues using equilibrium dialysis coupled to mass spectrometry or colorimetric outputs (Table S1, ESI†). For NrtA from *Synechococcus elongatus*, the affinities for nitrate (K_d = 0.32 μM) and nitrite (K_d = 0.34 μM) at 30 °C were comparable; however, for NrtA from *Phormidium laminosum* the affinity for nitrate (K_d = 2.0 ± 0.3 μM) was greater than that for nitrite (K_d = 3.8 ± 0.4 μM) at 45 °C.[29,30]

Given the similarities in the binding pocket of these homologues, we first used high-throughput differential scanning fluorimetry to determine if nitrate and nitrite could stabilize NrtA from *Synechocystis sp. PCC 6803* upon binding (Tables S1 and S2; Fig. S1–S5, ESI†).[31,32] The average unfolding temperature (T_m) of apo NrtA is 75.19 ± 0.18 °C in 20 mM HEPES at pH 7.5 with 100 mM NaCl. Titration with both nitrate and nitrite increases the T_m in a dose-dependent manner with saturation of binding, indicating the formation of a stable complex with NrtA. With respect to apo NrtA, the average ΔT_m increases by 3.72 ± 0.45 °C up to 15.74 ± 0.20 °C with 50 μM and 100 mM sodium nitrate, respectively. However, at the same concentrations of sodium nitrite, the average ΔT_m is smaller, 1.04 ± 0.65 °C and 12.42 ± 0.20 °C, suggesting a weaker complex. Similar results are not observed with sodium gluconate (ΔT_m < 1 °C), removing the possibility of ionic strength effects. To further support that nitrate and nitrite bind in the same pocket, we introduced the K269A mutation, which has been speculated to contribute to binding in a homologous bicarbonate transporter.[9,33] Under identical conditions, the T_m of apo NrtA K269A is 78.34 ± 0.50 °C, and no concentration-dependent stabilization occurs with nitrate, nitrite, or gluconate (ΔT_m < 1 °C), thus confirming that NrtA can bind both nitrate and nitrite using the same binding pocket (Fig. S6; Table S3, ESI†).

Building off this qualitative measure of recognition, we next employed ITC to quantify the binding affinities (K_d) and associated enthalpy and entropy contributions for both nitrate and nitrite.[34] At 20 °C in 20 mM HEPES at pH 7.7 with 50 mM NaCl, both ions undergo an exothermic binding reaction with a 1 : 1 stoichiometry (Fig. S7; Table 1 and Table S4, ESI†). Moreover, we verified that there is no proton uptake or release coupled to anion binding under these conditions by testing binding in buffers (*e.g.*, HEPES, sodium phosphate, Tris) with different ionization enthalpies (Fig. S8–S10; Table S4, ESI†).[35]

Table 1 Thermodynamic parameters for nitrate and nitrite binding to NrtA at different temperatures. All experiments were carried out in 20 mM HEPES with 50 mM NaCl at pH 7.7. The average of two protein preparations, each measured in duplicate with the standard deviation is shown

Anion	Temp. (°C)	K_d (nM)	ΔH (kJ mol^{-1})	$T\Delta S$ (kJ mol^{-1})	ΔG (kJ mol^{-1})
Nitrate	10	48 ± 8	−65.0 ± 0.7	−25.3 ± 0.5	−39.7 ± 0.4
	20	57 ± 23	−68.0 ± 1.2	−27.2 ± 1.7	−40.7 ± 1.0
	30	88 ± 9	−70.3 ± 2.5	−29.3 ± 2.3	−41.0 ± 0.3
	37	115 ± 8	−70.5 ± 1.2	−29.3 ± 1.2	−41.2 ± 0.2
Nitrite	10	187 ± 16	−56.3 ± 0.5	−19.8 ± 0.8	−36.5 ± 0.3
	20	230 ± 33	−60.6 ± 1.1	−23.4 ± 1.5	−37.3 ± 0.4
	30	473 ± 10	−63.5 ± 1.0	−26.8 ± 0.9	−36.7 ± 0.1
	37	753 ± 12	−69.7 ± 2.9	−33.3 ± 2.8	−36.4 ± 0.0

We next tested the effect of temperature on nitrate and nitrite binding from 10 to 37 °C (Fig. S7, S11–S13; Table 1 and Table S5, ESI†). Across this temperature range, the interaction between nitrate and NrtA is enthalpically favorable and entropically unfavorable with no significant differences in the Gibbs free energy ($\Delta G \approx -41$ kJ mol^{-1}) or corresponding thermodynamic parameters ($\Delta H \approx -68$ kJ mol^{-1}, $T\Delta S \approx -28$ kJ mol^{-1}). As expected, the binding affinity of nitrate for NrtA is weaker with increasing temperature and can be ranked as follows: 10 °C (K_d = 48 ± 8 nM) < 20 °C (K_d = 57 ± 23 nM) < 30 °C (K_d = 88 ± 9 nM) < 37 °C (K_d = 115 ± 8 nM). Compared to nitrate, the affinity of nitrite for NrtA is weaker at each temperature and can be ranked as follows: 10 °C (K_d = 187 ± 16 nM) < 20 °C (K_d = 230 ± 33 nM) < 30 °C (K_d = 473 ± 10 nM) < 37 °C (K_d = 753 ± 12 nM). This interaction is also enthalpically favorable and entropically unfavorable, but with a larger temperature dependent change in both thermodynamic parameters. From 10 °C to 37 °C, the ΔH for nitrite ranges from *ca.* −56 to −70 kJ mol^{-1} and $T\Delta S$ for nitrite ranges from *ca.* −20 to −33 kJ mol^{-1}. However, the Gibbs free energy ($\Delta G \approx -36$ kJ mol^{-1}) remains unchanged due to the enthalpy-entropy compensation.[36,37]

One noteworthy observation is that the ΔG for nitrate is ~5 kJ mol^{-1} more favorable than that for nitrite. It is possible that this difference is due to the entropic contributions to binding, particularly given that the enthalpic contributions are comparable for both anions at 37 °C. This can also be seen in the heat capacity change for nitrate (ΔC_p = −209 ± 45 J mol^{-1} K^{-1}) and nitrite (ΔC_p = −463 ± 96 J mol^{-1} K^{-1}). Since the ΔCp value can be linked to changes in the solvent-accessible surface area (SASA) of the protein, it is likely that NrtA undergoes a different structural rearrangement to bind each anion.[38,39]

To support these conjectures, we employed MD simulations for apo, nitrate, and nitrite-bound NrtA at 37 °C (Fig. 2 left panel; see Methods in ESI†).[40,41] Since we started with the crystal structure bound to nitrate, the one and two-dimensional root-mean-square deviation (RMSD) of the alpha carbon (Cα) atoms were used to determine when the apo and nitrite-bound NrtA finished adapting to their new environments (Fig. S14 and S15, ESI†). Therefore, 500 ns and 300 ns equilibrations were first performed for the apo and

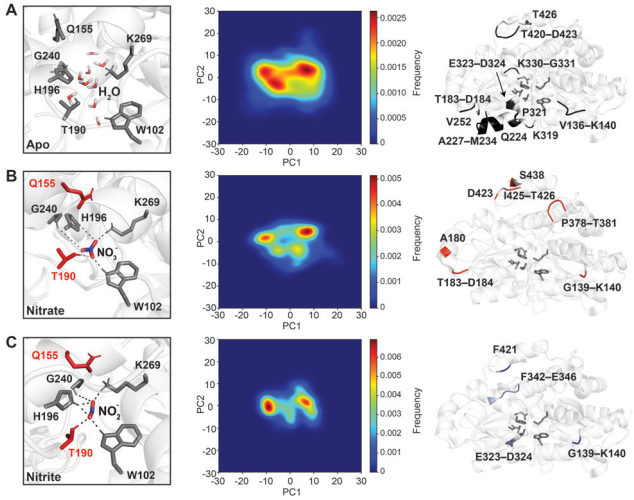

Fig. 2 Molecular dynamics (MD) simulations reveal that NrtA undergoes different conformational changes when bound to nitrate *versus* nitrite. Representative snapshot from the MD simulations (left), heatmap of the conformations sampled (middle), and residues that have Cα RMSF values greater than 0.4 Å along the PC1 direction (right) for (A) apo, (B) nitrate-bound, and (C) nitrite-bound NrtA. Polar residues as defined in Fig. 1 are shown as sticks in grey or red with hydrogen bonding or electrostatic interactions with the anions shown as dashed lines. Water, nitrate, and nitrite molecules are shown as sticks with all oxygen atoms in red, nitrogen atoms in blue, and hydrogen atoms in white. Each residue is labelled with the single letter amino acid abbreviation and corresponding sequence number. For the panels in the right column, all residues in the coloured regions are listed in Table S11 (ESI†).

anion-bound forms, respectively. This was followed by three independent production runs of 100 ns for each form. In all nine equilibrated trajectories, we first monitored distances within the nitrate binding pocket as defined in Fig. 1 (see also Fig. S16–S30, ESI†). In apo NrtA, water molecules transiently occupied the nitrate binding site (Movie S1, ESI†). In the bound forms, the distances between the nitrogen atom of each anion and Cα atoms of the coordinating residues W102, H196, G240, and K269 remain unchanged throughout the trajectories. Moreover, the shortest distances between the oxygen atoms of both anions and the closest atoms of the coordinating residues described above are maintained within 4 Å, which is in close agreement with the nitrate-bound crystal structure (Table S6, ESI†).[9] However, to our surprise, this is not the case with Q155. Since the sidechain rotates out of the binding pocket, the interactions between nitrate and nitrite with Q155 are at distances greater than 4 Å (Fig. S18 and S26, ESI†). This rearrangement is stabilized by water molecules and nearby residues, including N153, H196, E268, and K269 (Fig. S31, ESI†). To compensate, the hydroxyl group of T190 forms hydrogen bonding interactions (within 4 Å) with both anions (Fig. S19 and S27, ESI†). Likely due to these rearrangements, water molecules are also transiently found near the anions (Movies S2 and S3, ESI† for nitrate and nitrite, respectively). Together, these observations are unique to our MD simulations. In solution, it is likely that water molecules in the binding pocket of apo NrtA are displaced upon anion binding. Moreover, in the bound forms the binding pocket could be partially hydrated to enable anion sequestration or delivery to downstream proteins, NrtBCD.

We next investigated the global conformational changes upon anion binding from the MD trajectories. Dynamic cross-correlation matrix analysis (DCCM) shows that residues close to the binding pocket have anticorrelated motions in the two globular domains of apo NrtA (Fig. S32 and S33, ESI†; Supplement information.xlsx).[42] In the presence of nitrate or nitrite, the motions of the same residues are reduced (Fig. S32, ESI†).[43] Building off of this, principal component analysis (PCA) was employed.[44–46] The plots of the first and second principal components (PC1 *vs.* PC2) reveal that indeed apo NrtA has a wide distribution of conformational states (Fig. 2 middle panel, Fig. S34, ESI†). In the anion-bound forms, NrtA is shown to differentially redistribute its population of conformational substates sampled in the apo form.[47,48] This is also supported by the fact that the SASA of apo NrtA decreases with both nitrate (ΔSASA $\approx$ 485 Å^2) and nitrite (ΔSASA $\approx$ 787 Å^2) binding (Table S7, ESI†). Comparatively, the SASA for nitrite is less than nitrate (ΔSASA $\approx$ 302 Å^2), which is in line with the ΔC_p values described above.

To identify the residues that could contribute to these differences, root mean square fluctuation (RMSF) of the Cα atoms in the apo, nitrate, and nitrite-bound forms along the PC1 direction were plotted for three independent trajectories (Fig. S35, ESI†). To draw comparisons between all the datasets, only the residues that had Cα RMSF values greater than 0.4 Å and were common to all trajectories were selected (Fig. 2, right panel; Tables S8–S11, ESI†). For the apo form, we observed conformational flexibility at isolated residues and flexible loops, which include V136–K140, T183–D184, V252, K319, P321–D324, K330–G331, T420–D423, and T426. Interestingly, the helix (Q224, A227–M234) extending from the binding pocket residue P222 is found to have greater movement but is comparatively reduced in the anion-bound forms. However, we do observe conformationally flexibility in specific residues coupled to the binding of nitrate (A180, P378–T381, I425, and S438) and nitrite (F342–E346).

To summarize, we have presented the biophysical and *in silico* characterization of NrtA from *Synechocystis sp. PCC 6803* as a protein-based host for nitrate and nitrite. Thermodynamic analysis shows that NrtA recognizes nitrate with greater affinity than nitrite, with a $\sim$5 kJ mol^{-1} difference in the Gibbs free energy. Even though the binding is enthalpically favorable in both cases, it is plausible that differences between the two anions could arise from entropic contributions to binding and/or changes in the SASA of the protein. These conclusions are supported by our MD simulations that reveal how residues within the binding pocket rearrange in a similar fashion, while the global conformations differentially reorganize to accommodate each anion. Through our hybrid approach, we have begun to elucidate how NrtA can recognize anions with different physical properties in its biological context with extensions to general principles of anion binding proteins. Looking forward, we anticipate that the knowledge gained from our

investigations with NrtA and other biological supramolecular hosts could more broadly guide and enable the design of synthetic supramolecular hosts for aqueous anion recognition.

The authors thank Dr Gabriele Meloni, Dr John Sibert, and members of the Dodani Lab for helpful discussions. The authors also thank Dr Chad A. Brautigam and Dr Shih-Chia Tso (Macromolecular Biophysics Resource at UT Southwestern), Dr Yeun Hee Kim (Genome Center at UT Dallas), and Dr Christopher Simmons (Office of Information Technology at UT Dallas) for expert technical assistance. The authors acknowledge the Texas Advanced Computing Center (TACC) at UT Austin for providing HPC resources (http://www.tacc.utexas.edu). S.C.D acknowledges support from UT Dallas, the Welch Foundation (AT-1918-20170325, AT-2060-20210327), and the National Institute of General Medical Sciences of the National Institutes of Health (R35GM128923). This work is the sole responsibility of the authors and does not represent the views of the funding sources.

Conflicts of interest

There are no conflicts to declare.

Notes and references

1 X. Zhang, B. B. Ward and D. M. Sigman, *Chem. Rev.*, 2020, **120**, 5308–5351.
2 C. Moreno-Vivián and E. Flores, in *Biology of the Nitrogen Cycle*, Elsevier, 2007, pp. 263–282.
3 Y.-Y. Wang, Y.-H. Cheng, K.-E. Chen and Y.-F. Tsay, *Annu. Rev. Plant Biol.*, 2018, **69**, 85–122.
4 A. W. DeMartino, D. B. Kim-Shapiro, R. P. Patel and M. T. Gladwin, *Br. J. Pharmacol.*, 2019, **176**, 228–245.
5 E. A. Vidal, J. M. Alvarez, V. Araus, E. Riveras, M. D. Brooks, G. Krouk, S. Ruffel, L. Lejay, N. M. Crawford, G. M. Coruzzi and R. A. Gutiérrez, *Plant Cell*, 2020, **32**, 2094–2119.
6 M. Karwowska and A. Kononiuk, *Antioxidants*, 2020, **9**, 241.
7 A. Romanelli, D. X. Soto, I. Matiatos, D. E. Martínez and S. Esquius, *Sci. Total Environ.*, 2020, **715**, 136909.
8 X. Zhang, T. Zou, L. Lassaletta, N. D. Mueller, F. N. Tubiello, M. D. Lisk, C. Lu, R. T. Conant, C. D. Dorich, J. Gerber, H. Tian, T. Bruulsema, T. M. Maaz, K. Nishina, B. L. Bodirsky, A. Popp, L. Bouwman, A. Beusen, J. Chang, P. Havlík, D. Leclère, J. G. Canadell, R. B. Jackson, P. Heffer, N. Wanner, W. Zhang and E. A. Davidson, *Nat. Food*, 2021, **2**, 529–540.
9 N. M. Koropatkin, H. B. Pakrasi and T. J. Smith, *Proc. Natl. Acad. Sci. U. S. A.*, 2006, **103**, 9820–9825.
10 H. Yan, W. Huang, C. Yan, X. Gong, S. Jiang, Y. Zhao, J. Wang and Y. Shi, *Cell Rep.*, 2013, **3**, 716–723.
11 V. Niemann, M. Koch-Singenstreu, A. Neu, S. Nilkens, F. Götz, G. Unden and T. Stehle, *J. Mol. Biol.*, 2014, **426**, 1539–1553.
12 J. L. Parker and S. Newstead, *Nature*, 2014, **507**, 68–72.
13 C. Coelho and M. J. Romão, *Protein Sci.*, 2015, **24**, 1901–1911.
14 J. M. Fox, K. Kang, W. Sherman, A. Héroux, G. M. Sastry, M. Baghbanzadeh, M. R. Lockett and G. M. Whitesides, *J. Am. Chem. Soc.*, 2015, **137**, 3859–3866.
15 S. Horrell, D. Kekilli, R. W. Strange and M. A. Hough, *Metallomics*, 2017, **9**, 1470–1482.
16 D. Martín-Mora, Á. Ortega, M. A. Matilla, S. Martínez-Rodríguez, J. A. Gavira and T. Krell, *mBio*, 2019, **10**, e02334–18.
17 W. Yao, K. Wang, A. Wu, W. F. Reed and B. C. Gibb, *Chem. Sci.*, 2021, **12**, 320–330.
18 Y. Marcus, *Biophys. Chem.*, 1994, **51**, 111–127.
19 O. A. Okunola, P. V. Santacroce and J. T. Davis, *Supramol. Chem.*, 2008, **20**, 169–190.
20 R. Dutta and P. Ghosh, *Chem. Commun.*, 2015, **51**, 9070–9084.
21 Q. He, Z. Zhang, J. T. Brewster, V. M. Lynch, S. K. Kim and J. L. Sessler, *J. Am. Chem. Soc.*, 2016, **138**, 9779–9782.
22 S. S. R. Namashivaya, A. S. Oshchepkov, H. Ding, S. Förster, V. N. Khrustalev and E. A. Kataev, *Org. Lett.*, 2019, **21**, 8746–8750.
23 I. A. Rather, S. A. Wagay and R. Ali, *Coord. Chem. Rev.*, 2020, **415**, 213327.
24 J. N. Tutol, W. Peng and S. C. Dodani, *Biochemistry*, 2019, **58**, 31–35.
25 J. N. Tutol, H. C. Kam and S. C. Dodani, *ChemBioChem*, 2019, **20**, 1759–1765.
26 J. N. Tutol, J. Lee, H. Chi, F. N. Faizuddin, S. S. Abeyrathna, Q. Zhou, F. Morcos, G. Meloni and S. C. Dodani, *Chem. Sci.*, 2021, **12**, 5655–5663.
27 T. Omata, X. Andriesse and A. Hirano, *Mol. Gen. Genet.*, 1993, **236**, 193–202.
28 Y. Ohashi, W. Shi, N. Takatani, M. Aichi, S. Maeda, S. Watanabe, H. Yoshikawa and T. Omata, *J. Exp. Bot.*, 2011, **62**, 1411–1424.
29 S. Maeda and T. Omata, *J. Biol. Chem.*, 1997, **272**, 3036–3041.
30 D. Nagore, B. Sanz, J. Soria, M. Llarena, M. J. Llama, J. J. Calvete and J. L. Serra, *Biochim. Biophys. Acta*, 2006, **1760**, 172–181.
31 G. A. Holdgate and W. H. J. Ward, *Drug Discovery Today*, 2005, **10**, 1543–1550.
32 F. H. Niesen, H. Berglund and M. Vedadi, *Nat. Protoc.*, 2007, **2**, 2212–2221.
33 N. M. Koropatkin, D. W. Koppenaal, H. B. Pakrasi and T. J. Smith, *J. Biol. Chem.*, 2007, **282**, 2606–2614.
34 R. Perozzo, G. Folkers and L. Scapozza, *J. Recept. Signal Transduction*, 2004, **24**, 1–52.
35 R. N. Goldberg, N. Kishore and R. M. Lennen, *J. Phys. Chem. Ref. Data*, 2002, **31**, 231–370.
36 J. D. Chodera and D. L. Mobley, *Annu. Rev. Biophys.*, 2013, **42**, 121–142.
37 J. M. Fox, M. Zhao, M. J. Fink, K. Kang and G. M. Whitesides, *Annu. Rev. Biophys.*, 2018, **47**, 223–250.
38 N. V. Prabhu and K. A. Sharp, *Annu. Rev. Phys. Chem.*, 2005, **56**, 521–548.
39 S. Vega, O. Abian and A. Velazquez-Campoy, *Biochim. Biophys. Acta*, 2016, **1860**, 868–878.
40 W. Humphrey, A. Dalke and K. Schulten, *J. Mol. Graphics*, 1996, **14**, 33–38.
41 J. C. Phillips, D. J. Hardy, J. D. C. Maia, J. E. Stone, J. V. Ribeiro, R. C. Bernardi, R. Buch, G. Fiorin, J. Hénin, W. Jiang, R. McGreevy, M. C. R. Melo, B. K. Radak, R. D. Skeel, A. Singharoy, Y. Wang, B. Roux, A. Aksimentiev, Z. Luthey-Schulten, L. V. Kalé, K. Schulten, C. Chipot and E. Tajkhorshid, *J. Chem. Phys.*, 2020, **153**, 044130.
42 P. H. Hünenberger, A. E. Mark and W. F. van Gunsteren, *J. Mol. Biol.*, 1995, **252**, 492–503.
43 F. A. Quiocho and P. S. Ledvina, *Mol. Microbiol.*, 1996, **20**, 17–25.
44 N. Michaud-Agrawal, E. J. Denning, T. B. Woolf and O. Beckstein, *J. Comput. Chem.*, 2011, **32**, 2319–2327.
45 C. C. David and D. J. Jacobs, in *Methods Mol. Biol.*, Humana Press, NJ, 2014, vol. 1084, pp. 193–226.
46 R. Gowers, M. Linke, J. Barnoud, T. Reddy, M. Melo, S. Seyler, J. Domański, D. Dotson, S. Buchoux, I. Kenney and O. Beckstein, in *Proceedings of the 15th Python in Science Conference*, 2016, 98–105.
47 D. D. Boehr, R. Nussinov and P. E. Wright, *Nat. Chem. Biol.*, 2009, **5**, 789–796.
48 X. Du, Y. Li, Y.-L. Xia, S.-M. Ai, J. Liang, P. Sang, X.-L. Ji and S.-Q. Liu, *Int. J. Mol. Sci.*, 2016, **17**, 144.

